JGR Atmospheres

RESEARCH ARTICLE
10.1029/2025JD044365

Special Collection:
Land-atmosphere coupling: measurement, modelling and analysis

Toward Reconciling Bottom-Up and Top-Down Estimates of N_2O and CH_4 Emissions in Rotterdam

Xin Tong[1,2], Zhao Zhao[2], Arjan Hensen[3], Gerrit Jan Bruin[3], Steven van Heuven[1], Bert Scheeren[1], Ronald Hutjes[4], and Huilin Chen[1,2]

[1]Centre for Isotope Research (CIO), Energy and Sustainability Research Institute Groningen (ESRIG), University of Groningen, Groningen, The Netherlands, [2]Joint International Research Laboratory of Atmospheric and Earth System Sciences, School of Atmospheric Sciences, Nanjing University, Nanjing, China, [3]Netherlands Organisation for Applied Scientific Research (TNO), Petten, The Netherlands, [4]Earth Systems and Global Change, Department of Environmental Sciences, Wageningen University and Research, Wageningen, The Netherlands

Key Points:

- In situ measurements are used to reconcile top-down and bottom-up estimates of N_2O and CH_4 emissions in Rotterdam
- Top-down estimates of N_2O emissions are double the revised inventory, reducing the original inventory discrepancy by 50%
- Top-down and bottom-up estimates of CH_4 emissions do not show a significant difference within estimate uncertainties

Supporting Information:

Supporting Information may be found in the online version of this article.

Correspondence to:

H. Chen,
huilin.chen@nju.edu.cn

Citation:

Tong, X., Zhao, Z., Hensen, A., Bruin, G. J., van Heuven, S., Scheeren, B., et al. (2025). Toward reconciling bottom-up and top-down estimates of N_2O and CH_4 emissions in Rotterdam. *Journal of Geophysical Research: Atmospheres*, *130*, e2025JD044365. https://doi.org/10.1029/2025JD044365

Received 21 MAY 2025
Accepted 18 OCT 2025

Abstract Cities are key areas for implementing measures to reduce greenhouse gas emissions; however, large uncertainties exist in both "bottom-up" inventories and "top-down" estimates of urban N_2O and CH_4 emissions. We combine top-down and bottom-up approaches to evaluate the N_2O and CH_4 emission inventory for Rotterdam based on high-precision measurements made using an aircraft and a mobile vehicle. We divided the Rotterdam area into two sub-areas: (a) west industrial area (WIA) and (b) Rotterdam urban area (RUA). For the top-down estimate, the total emissions from Rotterdam are calculated as the sum of quantified emissions from both the WIA and the RUA based on aircraft observations. We further quantified emissions from key source categories including Wastewater Treatment Plants, Traffic and Transportation, Chemical Industry, Energy, and Refineries based on mobile vehicle and aircraft measurements. These measurements revealed that N_2O and CH_4 emissions were 2–4 and 4–16 times higher than inventory estimates, respectively. We revised the inventory after which the discrepancy between top-down estimates and Rotterdam's emission inventory decreased from approximately a factor of 4 to about 2 for N_2O, whereas CH_4 emissions between top-down and inventory showed no significant difference within the uncertainty. The persistent gap between top-down and bottom-up estimates implies the underestimation of N_2O emissions from other sources (such as sewerage and landfills) and/or the existence of missing sources that are not fully accounted for in the inventory. Our findings highlight the need for further comprehensive quantification across additional source categories and temporal scales.

Plain Language Summary Top-down and bottom-up estimates of urban N_2O and CH_4 emissions show inconsistencies and large uncertainties. To evaluate Rotterdam's emissions, we have made atmospheric N_2O and CH_4 measurements using both aircraft and mobile vehicle platforms, applying both top-down and bottom-up methods. Our results reveal that the inventory underestimates emissions from Sewerage and Wastewater Treatment Plants, Traffic and Transportation, Chemical Industry, Energy, and Refineries by factors of 2–4 for N_2O and 4–16 times for CH_4, respectively. The top-down estimates of Rotterdam's N_2O emissions are approximately 2 times the revised bottom-up inventory, and the discrepancy has decreased by 50% compared to the original inventory mainly due to revisions in industrial plant emissions, while CH_4 emission estimates show no significant difference within estimate uncertainties.

1. Introduction

Cities are significant sources of N_2O (Famulari et al., 2010; Järvi et al., 2014) and CH_4 (Helfter et al., 2016), but proper quantification and understanding of the emissions from complex infrastructures in urban areas are still scarce and usually require a combination of top-down (i.e., atmospheric inversions and micrometeorological methods) and bottom-up methods (i.e., inventories and process-based models). Inverse modeling can provide estimates for different emission source categories but remains very challenging for urban areas due to sparse availability of observation networks in cities and high computational requirements for fine resolution. Micrometeorological methods are more commonly used to determine urban emissions even though the estimated fluxes represent the integrated emissions from various kinds of sources without separating them. The aircraft mass balance approach (MBA) has been extensively used to quantify urban CH_4 emissions but is scarcely used for N_2O due to its relatively small signal-to-noise ratio. Among European cities, the CH_4 emissions estimated using the

MBA are larger than the inventory-based estimates for Berlin (Klausner et al., 2020) and London (O'Shea et al., 2014; Pitt et al., 2019) and consistent with the inventories for Utrecht, Groningen, and Rotterdam (Tong et al., 2023). To reconcile the gap if there is any, various emission sources need to be quantified individually at the source category level to derive a revised inventory for the comparison with top-down estimates.

The CH_4 emissions originate from diverse sources within the context of urban areas. The CH_4 emissions from natural gas leakage were detected at numerous spots in many American cities and can be estimated using the approach proposed and improved by (von Fischer et al., 2017; Weller et al., 2018, 2019), which requires concentration mapping of as many roads as possible. This approach has been gradually extended to quantify CH_4 emissions from other sources with isotopic composition measurements, such as the sewerage network systems and heating furnaces of buildings in European and Canadian cities (Defratyka et al., 2021; Fernandez et al., 2022). The facilities/plants in a city (i.e., landfills, wastewater treatment plants (WWTPs)) are also important emission sources and have relatively high emissions compared to aforementioned sources. Many studies have used airborne and ground-based measurements of downwind enhancements with an MBA or an inverse Gaussian plume model (IGM) approach to quantify N_2O and CH_4 emissions. In addition, vehicles have been reported to emit N_2O and CH_4 from exhausts, which have been quantified using an enhancement ratio method with CO_2 as a tracer based on the measurements in tunnels (Laskar et al., 2021; Nogueira et al., 2021; Popa et al., 2014; Wei & Wang, 2020).

The source patterns of urban CH_4 emissions vary among different countries/regions. In many cities in the U.S.A., natural gas leakage and fossil fuel usage contribute the largest part of total CH_4 emissions (Karion et al., 2023; Pitt et al., 2024; Sargent et al., 2021). However, in Canada, the waste category is the largest emitter for the Greater Toronto Area (Ars et al., 2020), whereas historical landfills and manholes are the top two largest sources for Montréal (Williams et al., 2022). In Europe, studies show different results for several cities. Natural gas systems emit the most CH_4 for Paris, Hamburg, and Utrecht (Defratyka et al., 2021; Maazallahi et al., 2020), whereas for Bucharest, wastewater is the largest emitter (Fernandez et al., 2022).

Compared to CH_4, N_2O emissions have been rarely studied on a city scale. Direct eddy covariance measurements based on tall towers were performed in Edinburgh (Famulari et al., 2010) and Helsinki (Järvi et al., 2014). (Famulari et al., 2010) found traffic-related emission calculations agreed well with measured N_2O fluxes, suggesting traffic is the major source; Järvi et al. (2014) found no seasonal change in N_2O fluxes from summer to autumn and that net emissions were slightly higher from the direction of vegetation than from the direction of road traffic. Quite a few top-down studies show that inventory-based N_2O estimates are 2–3 times underestimated for several cities in the U.S. (Addington et al., 2021; Herrera et al., 2021) and a European city (Tong et al., 2023). Point measurements in two European cities of Manchester (Barker et al., 2022) and Bristol (Charoenpornpukdee et al., 2023) suggested that nighttime N_2O emissions were associated with recreational use, but, without constraining information, it was impossible to estimate the emissions coming solely from recreational use.

Rotterdam is a complex industrial-urban area, the greenhouse gas (GHG) emissions of which have been rarely studied and reported. Super et al., 2017 estimated regional CO_2 fluxes using an MBA and found that the presence of point sources would complicate the flux estimation. In our previous work, we have found the estimated N_2O emissions in Rotterdam to be about 3 times the inventory-based estimates, but the estimated CH_4 emissions were consistent with the inventory (Tong et al., 2023). Here, we follow up on the previous work and aim to combine the top-down and bottom-up methods to evaluate the N_2O and CH_4 emissions in Rotterdam. We re-analyzed aircraft-based AirCore measurements made in our previous work and derived the top-down estimates for the entire Rotterdam area by including the industrial area's emissions. Using aircraft measurements and new mobile vehicle measurements made in this study, we estimated the emissions of specific source categories (Sewerage and Wastewater Treatment Plants, Traffic and Transportation, Chemical Industry, Energy, and Refineries) and used them to replace the reported emissions in the bottom-up inventory for revision. Finally, we compared the top-down estimates and the revised inventory.

2. Materials and Methods

We reconciled emission estimates for Rotterdam using both top-down and bottom-up methodologies. The top-down estimates were derived from an aircraft-based mass balance approach, whereas the bottom-up estimates were calculated based on a gridded emission inventory for key source sectors. Total emissions from the combined Refineries, Chemical Industry, and Energy sectors were quantified using the WRF-LES model coupled with airborne measurements. The emissions from WWTPs and Traffic & Transportation were determined using the

Table 1
Measurement Locations and Methodologies for Emissions Quantification

	Location/Source	Measurement	Quantification method
TOP-DOWN	WIA	Airborne measurements (enhancements over upwind background)	MBA
	RUA	Airborne measurements (Tong et al., 2023)	MBA (Tong et al., 2023)
BOTTOM-UP	Group categories (Refineries/ Chemical Industry/Energy)	Airborne measurements (enhancements above downwind background)	WRF-LES
	WWTPs	Ground-based mobile measurement	IGM
	Traffic and Transportation	Ground-based mobile measurement	Enhancement ratio

IGM approach and an enhancement ratio method, respectively, both based on ground-based mobile measurements. Detailed measurement locations and methodologies are summarized in Table 1.

2.1. Ruisdael-Rotterdam Campaign and Study Domain

The Ruisdael urban-atmosphere interactions intensive trace-gas and Aerosol measurement campaign (RITA) is aimed for measuring urban emissions of GHG and air pollution using atmospheric measurements. The RITA campaign took place in Rotterdam (Figure 1) with collaboration of various universities and scientific institutions in the Netherlands from August 22 to September 9 in 2022. We participated in the RITA-Rotterdam campaign and performed AirCore measurements aboard a lightweight aircraft for 4 days between August 30 and September 6 in 2022 (Tong et al., 2023) referred to as flight 0830, 0901, 0905, and 0906 (mmdd). TNO operated an instrumented van and trailer for mobile GHG measurements throughout the city. We used both airborne and mobile ground-based measurements for emission estimation in this study.

The study domain encompasses the area covered by the trajectory of flight 0906 (Figure 1b), which includes the municipality of Rotterdam and several neighboring municipalities. Rotterdam, located in the western Netherlands along the North Sea coast, is the country's second-largest city and home to Europe's largest seaport. Based on the aircraft flight transects, we divided the study domain into two sub-areas: the West Industrial Area (WIA) and the Rotterdam Urban Area (RUA) (Figure 1b). The WIA encompasses the industrial zone in the western portion of the domain, bounded by two parallel flight transects. The RUA covers the remaining eastern portion of the study domain. It should be noted that the boundary between WIA and RUA is not rigidly defined, as flight trajectories varied slightly between measurement days. However, the summed emissions from both subareas (WIA + RUA) represent the total emissions from the entire Rotterdam study domain.

2.2. The Emission Inventories of N_2O and CH_4 for Rotterdam

The prior emissions of N_2O and CH_4 for the Rotterdam area come from the Dutch national inventory, which is reported every year and does not have a significant interannual variability since 2019. The inventory with 13 categories was compiled first on a national scale and was then allocated to different spatial scales such as

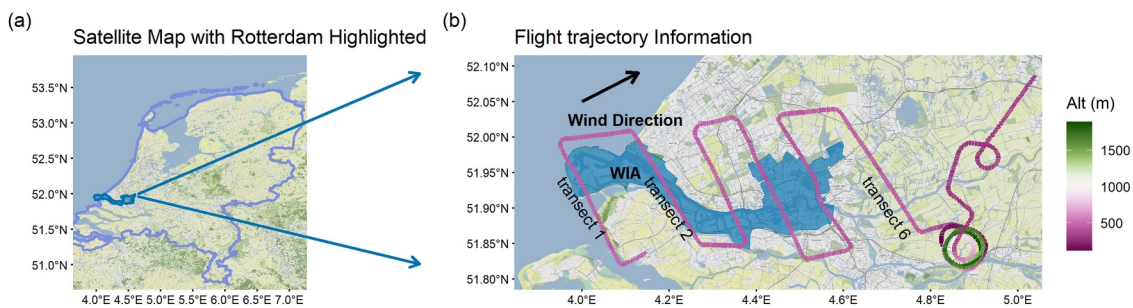

Figure 1. The studied Rotterdam area painted by blue color and the trajectory of flight 0906. The colorbar indicated the flight altitude above the ground level, the arrow indicates average wind direction below the convective boundary layer height, and the industrial area enclosed by the transects 1 and 2 in the west is named by WIA in this study.

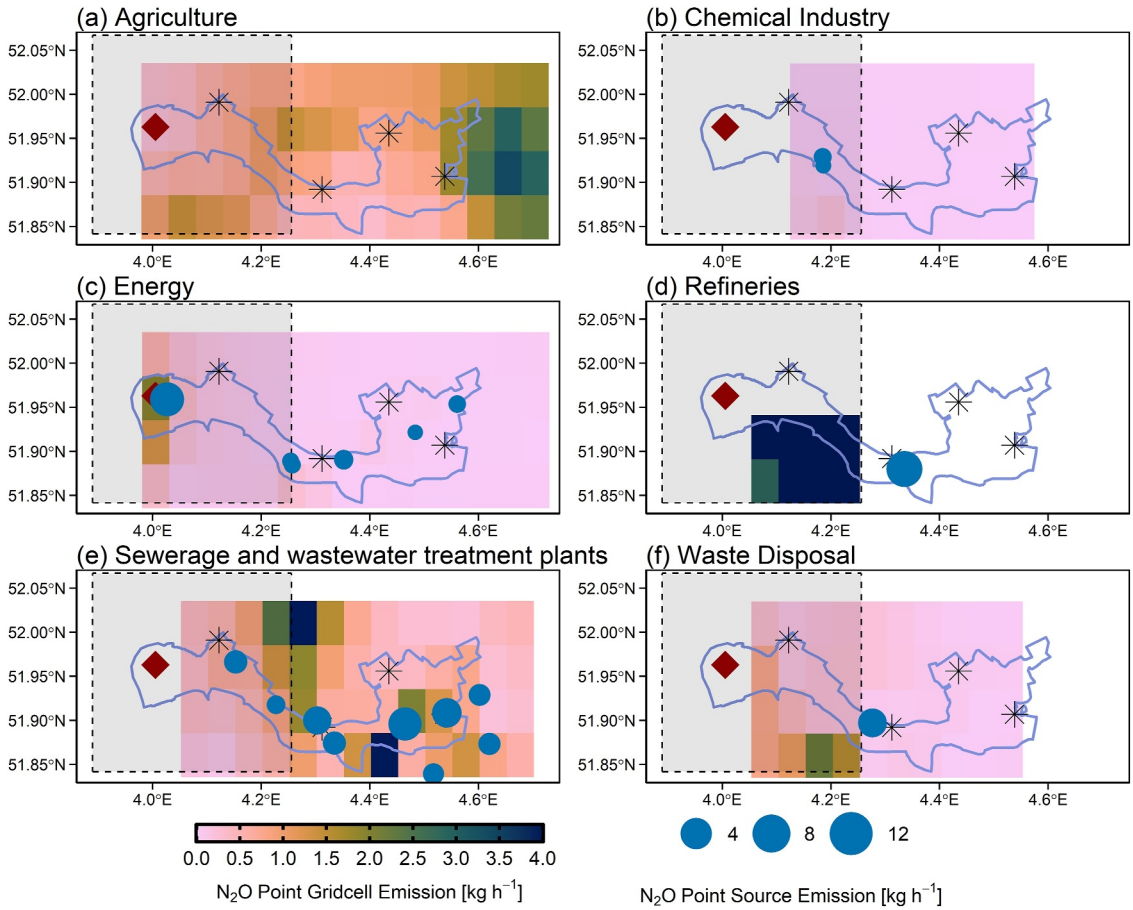

Figure 2. The 5×5 km^2 Dutch gridded emission inventory for N_2O, taking key six source categories as examples. The area in the rectangular box bounded by the dashed line indicates the study domain simulated by the WRF-LES model, the solid circles indicate point sources, and the diamond indicates the location of the mast with vertical profile measurements of meteorological parameters, and the star sign indicates the four KNMI stations with wind measurements.

province, municipality, and 5×5 km^2 grid cells. In our study, we have revised the 5×5 km^2 gridded emission inventory. The emission of each grid cell is the sum of the allocated emissions for point and diffuse sources. Because locations and emissions of point sources were registered and can also be found in the Dutch government website, although diffuse sources' emissions are unknown, we derived them by subtracting point sources' emissions from the gridded emission inventory. The spatial allocation depends on the category-dependent proxies for diffuse sources and the specific locations for point sources. Most categories consist of both point and diffuse sources, but the categories of agriculture, nature, consumers, and drinking water supply contain diffuse sources only, and the Refineries category includes point sources only. As shown in Figure 2, the category of Refineries only has emissions for the grid cells in which the point sources are located, whereas other categories such as Sewerage and Wastewater Treatment Plants have emissions for most grid cells. The spatial allocation of the emissions from Sewerage and Wastewater Treatment Plants includes both the locations of WWTPs and the proxy inhabitants for sewerage systems (diffuse sources). Most categories have less than 4 proxies, but the categories of Agriculture and Traffic and Transportation have 7 and 12 proxies, respectively, for spatial allocation. A more detailed descriptions of the Dutch national inventory is presented in the Text S1 in Supporting Information S1.

In this study, we focused on improving the emissions estimates for the source categories of Sewerage and Wastewater Treatment Plants, Traffic and Transportation, Chemical Industries, Energy, and Refineries. Each category's N_2O and CH_4 emissions were presented separately for point and diffuse sources regarding the whole Rotterdam area (Figure S1 in Supporting Information S1). The category of Sewerage and Wastewater Treatment Plants ranked as the 2nd and the 4th largest category for the emissions of N_2O and CH_4, respectively; the emissions from point sources (WWTPs) and diffuse sources (sewerage systems) are nearly equal. WWTPs and the industrial plants categorized into the aforementioned source categories are main point sources for both N_2O

and CH_4 (Figure S1 in Supporting Information S1). The category of Traffic and Transportation ranked 4th and 6th for the emissions of N_2O and CH_4, respectively, and total emissions are dominated by diffuse sources' emissions.

2.3. Airborne Quantification of WIA Emissions Using MBA

We performed aircraft-based AirCore measurements over Rotterdam in our previous work (Tong et al., 2023). The aircraft-based AirCore is a portable sampling system for continuous sampling of air along the flight trajectory. The air sample, collected in a very long and thin tube, remains largely un-mixed with itself and can be used for the subsequent measurements of multiple trace gases. So far, the air sample has been measured by two cavity ring-down spectroscopy analyzers (Picarro, Inc.) in series or single quantum cascade laser spectrometer (Aerodyne Research Inc.) for simultaneous measurements of N_2O and CH_4. More details about the AirCore measurements can be found in Tong et al. (2023). The mass-balance estimates of Rotterdam presented in our previous work (Tong et al., 2023) did not include the emissions from the WIA because the background for mass-balance estimation was selected as the concentrations downwind rather than upwind the WIA. In this study, we extended the previous work by conducting an MBA to estimate N_2O and CH_4 emissions from the WIA and added them to the emissions estimated in our previous study to represent the total emissions in Rotterdam.

We re-analyzed the measured atmospheric concentrations of N_2O and CH_4 for four flights in 2022. As shown in Figure 3, four flights show clear concentration enhancements relative to either the mean concentrations of the upwind transect or the concentrations at both sides of the downwind transect for N_2O, while only one flight 0906 for CH_4 (Figure S2 in Supporting Information S1). The prevalent wind direction for flight 0906 came from the sea but for the other three flights came from inland (Figure S3 in Supporting Information S1). CH_4 emissions from the WIA may be not large enough to cause a signal significantly distinguished from the high upwind concentrations that were already elevated by strong inland emissions, such as massive CH_4 from the glasshouse horticulture area between the WIA and The Hague (Super et al., 2017).

We selected upwind concentrations as the background that was to be subtracted from the downwind plumes, in order to derive enhancements, based on which we determined the regional emissions in the WIA for three individual flights 0830, 0901, and 0906 for N_2O, excluding flight 0905. Flight 0905 was not suitable for the application of the MBA because (a) the upwind concentrations have missing values, and (b) the downwind plume is not isolated from the adjacent plume to the east (Figure 3), which makes the determination of plume width rather difficult. The relative uncertainty of estimated fluxes was determined as the root mean square of the relative uncertainties of concentration enhancements, wind direction, wind speed, plume width, and the planetary boundary layer (Tong et al., 2023). The footprint of the estimated emissions utilizing upwind concentrations as background can be approximately defined by the area enclosed between the upwind and downwind transects.

2.4. Point-Source Emissions Estimation Based on WRF-LES Model and Airborne Observations

In recent years, large eddy simulation (LES), for example, driven by the Weather Research and Forecasting (WRF) Model has been used to estimate point sources' emissions (Caulton et al., 2018; Ražnjević et al., 2022; Saide et al., 2018). The principle of estimating emissions is to compare the concentration enhancements caused by unknown emission sources with those caused by the sources with known emission rates, assuming plumes disperse and transport under the same atmospheric conditions for both known and unknown sources. The enhancements caused by known sources can be measured or modeled for those emission estimation methods following this principle. For example, in controlled-release experiments, the enhancements caused by known sources are measured, whereas in the IGM method, they are modeled. Moreover, the enhancements caused by unknown sources are commonly measured based on multiple platforms (mobile vehicle, aircraft, and satellites). More details about the associated equation are shown in the Text S3 in Supporting Information S1.

In this study, we used the enhancements modeled by the WRF-LES model against airborne measurements to estimate the emission rates of the upwind point sources in the WIA, as shown below:

$$Q = \frac{\sum c_{\mathrm{meas}} \times u_{\mathrm{meas}}}{\sum c_{\mathrm{LES}} \times u_{\mathrm{LES}}} \times Q_{\mathrm{LES}} \quad (1)$$

Here, Q is the emission rate of unknown sources (in kg hr^{-1}), Q_{LES}, c_{LES}, and u_{LES} are the known source emission rate, the integrated modeled concentration enhancements along a transect, and the modeled wind speed,

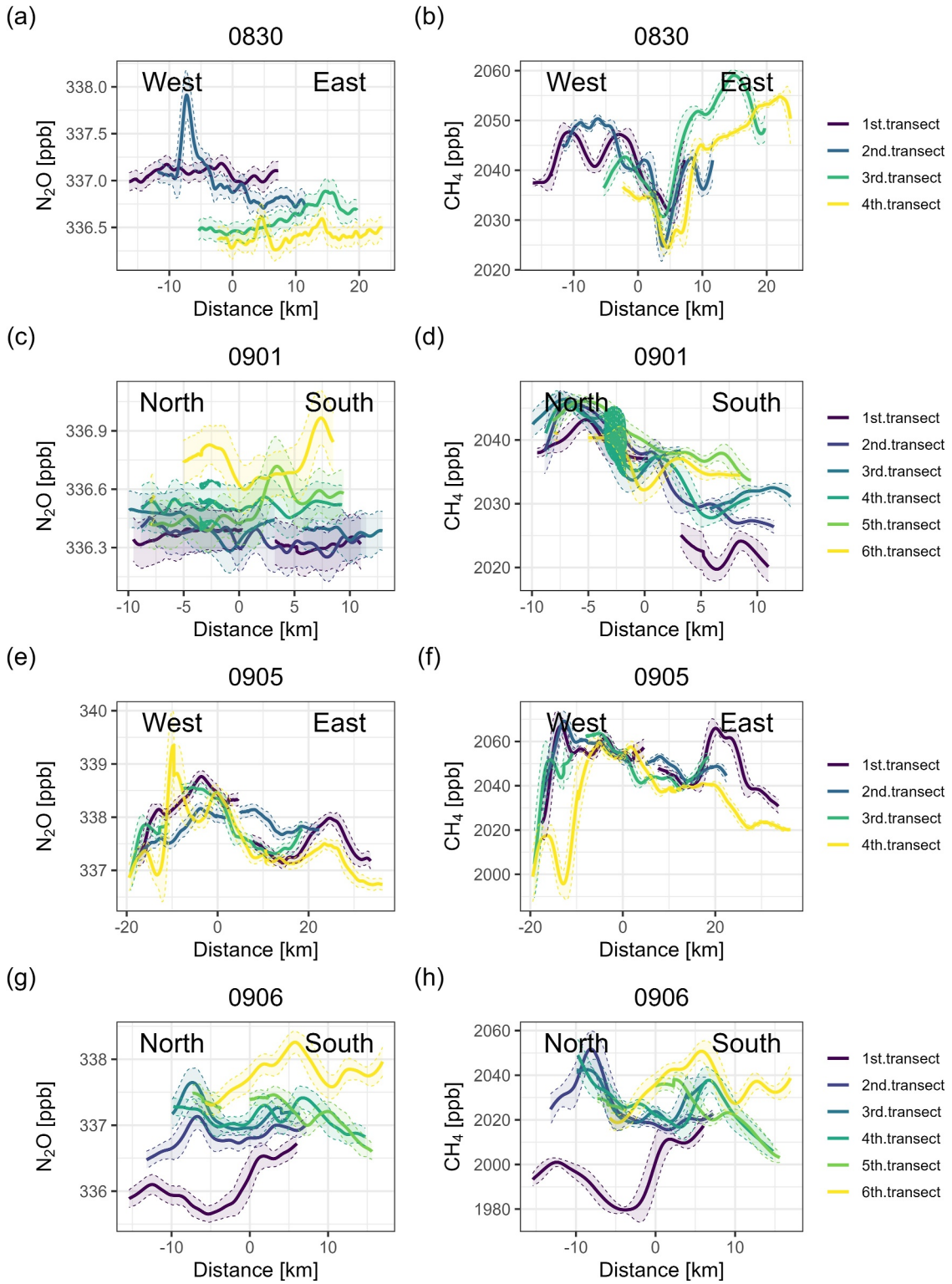

Figure 3. The mole fraction of N_2O and CH_4 along the projected transects that are perpendicular to the wind direction during flights (a, b) on August 30, (c, d) on September 1, (e, f) on September 5, and (g, h) on September 6. The distance is determined from arbitrary zero points on the projected transects to the measurement points. Horizontal transects were conducted at the same altitude and are sequentially numbered (upwind to downwind) from one to four or six depending on the flight. The distance from negative to positive values represents either west-to-east or south-to-north movement depending on the flight's trajectory on each specific day. The lines show Gaussian-smoothed data using a 1-min weighted moving average window on second-by-second measurements, whereas the shaded area represents the standard deviation of values within each smoothing window.

respectively; c_{meas} and u_{meas} indicate the same meanings but for airborne measurements. The WRF-LES model directly simulates concentration enhancements from point sources, whereas airborne measurements require deriving these enhancements by subtracting background concentrations measured at the lateral edges of downwind transects. Although downwind background concentrations exceed upwind background levels due to regional emissions throughout the study area, the observed downwind plume exhibits a narrow spatial structure (approximately 5 km width) that is characteristic of point source emissions rather than diffuse regional sources. Given the relatively large spatial scale of the study area compared to the narrow plume width, the observed concentration enhancements are attributed primarily to upwind point sources, and therefore enhancements calculated by subtracting the downwind background concentrations are considered representative of point source emissions and suitable for emission rate quantification while accounting for the regional emission background present in the study area.

The WRF-LES simulation employs a domain of 12 km × 17 km (gray area in Figure 2) with 30 m horizontal resolution. This configuration allows a realistic representation of multiple emission sources while adequately resolving turbulence between sources and observation points, maintaining computational efficiency. The vertical structure contains 141 levels ranging from approximately 5 m thickness at the surface to 170 m thickness in the upper layers with the model top at 2 km altitude. The model spun up for 2 hr before analysis to simulate a mixed convective boundary layer.

The estimated N_2O and CH_4 emissions based on the WRF-LES model represented the calculated total emissions of the placed point sources. We set up four emission point sources (representing one power plant, one refinery, and two chemical industries) in the WRF-LES model, which were reported in the Dutch emission inventory of N_2O and located upwind of where the downwind enhancements were observed on flight transects. Assuming CH_4 experiences the same atmospheric transport as N_2O does, the modeled plume in unit of kg kg^{-1} can be converted to concentration enhancements in unit of ppb for either N_2O or CH_4. More information about model configuration is presented in the Text S3 in Supporting Information S1. The observed plumes for the three flights 0830, 0901, and 0906 are examined to be comparable with the modeled plume. The premise of application of the aforementioned concept is that observed plumes should be attributed to the emissions from the same known sources set up in the WRF-LES model. The three flights show plumes with widths ranging from 5 to 10 km, which is a logical range for the plume caused by point sources according to the simulated plume by the WRF-LES model and the reported plume width in literature (SI). However, flight 0905 shows a plume with a width of around 20 km at a downwind distance of about 3 km, which is most likely due to regional emissions rather than point sources' emissions.

2.4.1. WRF-LES Model Validation With Tower Data

Implementing the method mentioned above relies heavily on understanding how CH_4 plumes behave in the atmosphere. Realistic turbulence representation is essential because turbulent eddies control the mixing and dilution of CH_4 plumes. If the WRF-LES model doesn't accurately represent the real atmospheric conditions, the resulting emission estimates will be biased regardless of how sophisticated the inverse modeling technique or how precise the concentration measurements are. This makes realistic model configuration essential for credible CH_4 emission quantification.

To evaluate if the WRF-LES model adequately represents atmospheric conditions, we compared modeled meteorological parameters with measurements from a meteorological tower located within the simulation domain (Figure 2). The tower provides measurements at four height levels (25, 80, 126, and 135m above ground level) using cup anemometers and wind vanes for horizontal wind components. We obtained 10-min time series data from September 1st to 7th and compared them with modeled data for the three flight days (0901, 0905, and 0906). Output variables from the WRF-LES grid cell closest to the tower location were extracted from the corresponding vertical levels.

The WRF-LES model well reproduced observed air and potential temperatures (Figure S4 in Supporting Information S1) with mean absolute errors less than 0.4 to 3 K for individual days. To assess the model's representation of atmospheric mixing, we calculated turbulence intensity (TI), which is defined as the ratio of wind speed standard deviation to mean wind speed, for both measurements and model output (Manwell et al., 2009). The simulated TI is overall underestimated compared to measurements with the absolute difference ranging from 5% to 12.5% across the three flight days. The differences between modeled and observed wind directions ranged

from 20° to 70°, whereas temperature validation and TI analysis suggest the WRF-LES model captures essential atmospheric mixing processes.

2.4.2. Sensitivity Test

We have done a sensitivity test to study the impact of various combination of different options involved in the two procedures for concentration enhancement calculation (Figure S5 in Supporting Information S1). Since the output of the WRF-LES model is in 3-dimension, we need to extract the grids to match one dimensional flight trajectories (Tong, 2025). For each moment (per output) simulated by the WRF-LES model, grid cells were extracted by the means of (a) selecting the single grid cell that is closest to the location of the aircraft at the same timestamp (the number of selected grid cells for a flight is equal to the time steps of the WRF-LES model output) and (b) selecting the grid cells where downwind transects were flown for the entire period (Figures S5 and S6 in Supporting Information S1). The first way results in only one plume, but the second way leads to plenty of instantaneous plumes for each flight, which were averaged for different periods (the entire simulation period, and 2, 5, 10, and 20 min). Taken together, it aggregated to 14 matches in total, a combination of seven types of the plumes (one plume from the first extraction method, instantaneous plumes, averaged plumes for 5 different time periods) and two types of smoothing functions of "spline" and "loess."

We chose estimates based on the match of the "spline" function and the plume averaged from the entire simulation period to represent emissions, although we presented individual matches. The first extraction method and the second method using the plume average yield one estimate per smoothing function match. For the second method using instantaneous plumes, there are many estimates, so we determined both mean and median (Figure S9 in Supporting Information S1). Smoothing functions and extraction methods similarly impacted N_2O emissions for flight 0830 but were more sensitive for flights 0901 and 0906. We decided to use the second extraction method with plume averaging over the whole simulation period because the first method does not account for atmospheric variabilities and instantaneous plumes yielded high outliers. Following similar studies, we used the plume averaged over about half an hour to determine emissions. We decided to use the "spline" function to smooth both observed and modeled plumes based on its good fitting performance by visual inspection.

2.5. Mobile Survey

2.5.1. Mobile Ground-Based Measurements

Mobile surveys using an instrumented vehicle were performed by TNO in the Rotterdam area from August 23 to September 7 in 2022. The vehicle drove primarily on the outermost circular road around Rotterdam, went through tunnels, and passed by WWTPs and industrial facilities in Rotterdam (Figure S11 in Supporting Information S1). We focused on the WWTPs in the RUA that had sufficient available transects. The concentration measurements were performed at a sampling height of 3 m, which is in front of the vehicle to avoid impact of the vehicle exhaust. In this campaign, a tunable infrared laser direct absorption spectroscopy (TILDAS) dual laser trace gas analyzer (Aerodyne Research, Inc. Billerica, USA) was used, which enables the simultaneous measurement of multiple species (CH_4, C_2H_6, N_2O, CO, CO_2, H_2O). This system has a 1-σ precision (1 Hz) of 2.4, 0.1, 0.1, 2.5 ppb and 0.4 ppm for CH_4, C_2H_6, N_2O, CO, and CO_2, respectively. In addition, instrument calibrations were conducted at the start and end of the measurement days with calibration gases measured against WMO-certified standards at the Cabauw tall tower atmospheric measurement station in the Netherlands.

2.5.2. The Emissions From Waste Water Treatment Plants

An inverse Gaussian dispersion plume model (IGM) was employed to optimize emission rates by matching modeled and observed atmospheric concentration enhancements with the match evaluated through quantitative metrics (enhancement areas) or within a Bayesian inversion framework. Under steady-state atmospheric conditions with constant wind speed and direction, downwind concentration enhancements from point sources follow a Gaussian distribution function described as follows:

$$c(x,y,z) = \frac{Q}{2\pi\sigma_y\sigma_z u} e^{-0.5*\left(\frac{y}{\sigma_y}\right)^2} \left(e^{-0.5*\left(\frac{z-h}{\sigma_z}\right)^2} + e^{-0.5*\left(\frac{z+h}{\sigma_z}\right)^2} \right) \quad (2)$$

where x represents the downwind distance from the source [m], y indicates the distance perpendicular to wind direction [m], z denotes the measurement height [m], h indicates the source height [m], u represents wind speed [m·s^{-1}], Q indicates the emission rate, and c represents downwind concentrations. The dispersion parameters σ_y and σ_z were determined using an empirical equation for urban environments with Pasquill–Gifford's stability class scheme (USEPA, 1995) as shown in Table S7 in Supporting Information S1. Using mobile measurements and the IGM approach, we quantified emissions from 3 WWTPs for N_2O and 4 WWTPs for CH_4, subsequently upscaling these quantified emissions using the relationship between quantified and inventory estimates to represent total emissions from 9 WWTPs in the Rotterdam area. We did not use the WRF-LES model as it demands extensive computational time and resources for high-resolution simulations. The IGM methodology simulates downwind enhancements caused by known emission rates (Q_{model}), which are set to 1 g·s^{-1}, and compares them with measured plumes to infer actual emission rates Q as described by Equation 3,

$$Q = Q_{\text{model}} \cdot \frac{\int C_{\text{observe}}}{\int C_{\text{model}}} \tag{3}$$

where the integrals of areas bounded by concentration enhancements along the y (perpendicular to wind direction) and z (vertical direction) axes are matched between modeled, $\int C_{\text{model}}$, and observed values, $\int C_{\text{observe}}$. Detailed application of this approach is provided in Text S4 in Supporting Information S1.

We only present the quantified emissions from WWTPs, excluding other industrial plants (refineries, power plants, and chemical plants) due to limited available transects. After performing data screening and quality control, we obtained a list of plumes that were determined to be caused by point source emissions rather than the incomplete combustion of fossil fuel from road vehicles (Table S6 in Supporting Information S1). The major uncertainties in the estimated emission rates derived by the IGM are caused by the atmospheric variables, wind speed, and the selection of stability class (Caulton et al., 2018; Moore et al., 2023). To minimize the uncertainty of atmospheric variability, (Caulton et al., 2018) recommended having at least 10 sampling transects. The WWTP Kralingseveer was sampled at least 10 times for measurements of both N_2O and CH_4, whereas other plants were sampled one to two times. A key challenge in mobile atmospheric measurements is successfully intercepting the plumes downwind emission sources. The detectability of elevated emissions depends on vertical plume dispersion, which determines whether pollutants reach ground-level measurement heights. When the vertical dispersion parameter (σ_z) exceeds the source height, plumes disperse sufficiently to reach the surface, enabling detection if concentration enhancements surpass both background variability and instrument detection limits.

In this study, N_2O emissions from industrial facilities originate from both ground-level sources and elevated stacks tens to hundreds of meters high. Although ground-level emissions are readily detectable, elevated stack emissions present detection challenges that depend on three critical factors: (a) downwind sampling distance, (b) atmospheric stability conditions, and (c) measurement precision. The vertical dispersion parameter σ_z varies significantly with atmospheric conditions even at fixed downwind distances, meaning sampling transects may fail to intercept plumes when σ_z becomes much smaller than the source height. At a representative 1,000 m downwind distance, typical stability classes (B, C, D) yield σ_z values of 123 m, 170 m, and 200 m, respectively. The variation demonstrates that emission quantification becomes highly uncertain when atmospheric conditions result in insufficient vertical mixing relative to source height.

2.5.3. Wind Measurements

The surface wind was measured still per minute at the "Van Brienenoord" site during the RITA-Rotterdam campaign, and it was compared with the wind measured at approximately 10 m a.g.l. from three KNMI stations. The hourly data sets for each station (https://www.knmi.nl/nederland-nu/klimatologie/uurgegevens) were used for analysis in this study. The KNMI station "Hoek van Holland" is close to the coastline in the west, the station "Geulhaven" is located in the middle areas of Rotterdam, and the station "Rotterdam" is located inland close to Rotterdam airport (Figure 2). The wind direction near the coastline is on most days different from the wind measured from the other two stations far away from the coastline. The mean wind speed per day near the coastline is almost a factor of 2 larger than that of/at the other two stations (Figure S12 in Supporting Information S1). Throughout the mobile measurement campaign, wind directions at the four monitoring stations varied extensively spanning from 25° to 300°. Additionally, significant wind direction changes occurred within single

days for each station, indicating highly variable meteorological conditions. Since wind conditions vary across different locations, we selected wind data measured closest to the targeted point sources to determine the stability class and identify the downwind direction. Once the downwind direction was determined, the actual wind direction was refined using the IGM approach for emission estimation by considering the direction from the source location to the observed peak of the plumes.

2.5.4. Vehicular Emissions

The mobile measurements exhibited the plumes of N_2O and CH_4 in the tunnels in Rotterdam, and we determined the N_2O and CH_4 emissions from the category of Traffic and Transportation using the enhancement ratios of $\frac{\Delta N_2O}{\Delta CO_2}$ and $\frac{\Delta CH_4}{\Delta CO_2}$ measured from various tunnels (Figure S13 in Supporting Information S1). With the CO_2 inventory emission of 3.82×105 kg hr^{-1} for Traffic and Transportation obtained from the Dutch national emission registration data base (https://data.emissieregistratie.nl/export), the emissions of N_2O and CH_4 were estimated as a product of CO_2 inventory emissions and the measured enhancement ratios of $\frac{\Delta N_2O}{\Delta CO_2}$ and $\frac{\Delta CH_4}{\Delta CO_2}$ using the following equation:

$$E_{N_2O(CH_4)} = \frac{\Delta N_2O(CH_4)}{\Delta CO_2} \times E_{CO_2} \quad (4)$$

where $\frac{\Delta N_2O(CH_4)}{\Delta CO_2}$ is the enhancement ratios of $\frac{\Delta N_2O}{\Delta CO_2}$ and $\frac{\Delta CH_4}{\Delta CO_2}$, and E_{CO_2} is the inventory estimates of CO_2 emissions from the category "transportation and traffic" for the Rotterdam area.

This category largely consists of diffuse sources (Figure S1 in Supporting Information S1), and it is not possible to purely quantify their emissions without extra constraining information. Sampling in tunnels is more concentrated and avoids the perturbation of external sources. Enhancement ratios were determined from the slopes of linear regressions between N_2O-CO_2 and CH_4-CO_2 across 19 plume measurements from multiple tunnels. To ensure statistical reliability, we applied selection criteria requiring R-squared values $\geq$0.4 and a minimum of two qualifying plumes per location. Enhancement ratios meeting these criteria were then averaged.

2.6. The Comparison of the Top-Down Estimates and the Revised Bottom-Up Inventory

The Dutch government published a provisional inventory online for year t in the summer of year $t + 1$ and updated it at the end of year $t + 1$ or the beginning of year $t + 2$. The final emissions may also be different from the provisional emissions as they are adjusted because of methodology changes or error corrections (https://www.emissieregistratie.nl/data/datacorrecties). In this study, we presented the Dutch emission inventory of N_2O and CH_4 with two versions, an updated version and the provisional version, that was analyzed in our previous work (Tong et al., 2023). The updated Dutch inventory shows higher emissions than the provisional version does for N_2O (Figure S1 in Supporting Information S1) while not significantly for CH_4 (Figure S1 in Supporting Information S1). The total N_2O emissions from the category Sewerage and Wastewater Treatment Plants in the provisional version of the Dutch inventory was smaller than those from point sources (WWTPs). This explains why the subtracted N_2O emissions of diffuse sources were negative (Figure S1 in Supporting Information S1). In the updated version, total N_2O emissions from Sewerage and Wastewater Treatment Plants have been adjusted, resulting in a positive subtracted number of diffuse sources. This change contributed the most to the increased N_2O emissions in the updated version compared to the provisional version. In addition, CH_4 emissions decreased for the diffuse sources under the categories of Nature and Sewerage and wastewater treatment plants but increased for Agriculture and Consumers.

We established a revised inventory based on the updated version of the Dutch inventory for both N_2O and CH_4. We replaced the emission estimates reported in the inventory with the new emission estimates in this study for the source categories of Sewerage and Wastewater Treatment Plants, Traffic and Transportation, Chemical Industry, Refineries, and Energy. We only updated the point sources' emissions (WWTPs) and did not change the diffuse sources' emissions (Sewerage) under the category of Sewerage and Wastewater Treatment Plants as we do not have enough data to quantify the emissions from sewerage. We updated the emissions from the category Traffic and Transportation with the emissions quantified from tunnels as this category's emissions are predominantly

Table 2
The Total Point Source Emissions of N_2O and CH_4 From the Upwind Industrial Plants Located in the WIA Estimated by the WRF-LES Model for Individual Flights With Uncertainties for Individual Days Reported as the Range of the Estimated Emissions in the Sensitivity Test

Species	Flight	Emission rate [kg h^{-1}]
N_2O	0830	139 [101, 190]
	0901	30 [25, 53]
	0906	41 [31, 56]
CH_4	0906	1,669 [1,183, 2040]

diffuse. Taking the categories of Chemical Industry, Energy, and Refineries as a group, we updated the emissions from the point sources in the WIA with the new estimated emissions using the WRF-LES model, and the emissions from the RUA did not change.

To determine uncertainty of top-down estimates, we took the square root of the sum of the squares of the uncertainties of the emissions from the WIA and the RUA. The uncertainties of the Dutch inventory estimates used here were determined to be the mean of the total uncertainties considering all emissions categories which were calculated by two methods (standard error propagation and Monte Carlo analysis) as reported in the national inventory report (van der Net et al., 2024).

3. Results and Discussions

3.1. The Emissions From Industrial Plants

The estimated emissions represent the total emissions from all the upwind industrial plants (point sources) in the WIA without differentiating between various source categories (Chemical Industry, Energy, and Refineries). We presented the estimated emissions on three individual days for N_2O and single day for CH_4 (Table 2). The N_2O emission for the day 0830 is several times the emissions for the other days, which do not significantly differ from each other. We used the mean of estimated emissions on three individual days to represent N_2O emissions from the source category group in the WIA.

We replaced the inventory estimates for the point sources' emissions under the category group in the WIA with the new estimates to derive an updated estimate, whereas the emissions in the RUA remain the same. We find that the estimated emissions are about 3 and 16 times the inventory estimates for N_2O and CH_4 (Figure 4). Studies have found quite similar results that CH_4 emission rates were 21–120 and 11–90 times the facility-reported estimates for power plants and refineries (Lavoie et al., 2017).

3.2. The Emissions of N_2O and CH_4 From WWTPs

There are in total 9 WWTPs in the Rotterdam area, but only half of them were investigated using mobile measurements. The WWTP Kralingseveer has in total more than 10 plume measurements for both N_2O and CH_4 during the campaign. In contrast, only one or two plumes were observed downwind of the individual WWTPs Barendrecht, Ridderkerk, and Rozenburg (for CH_4 not for N_2O), the emissions of which were quantified using an

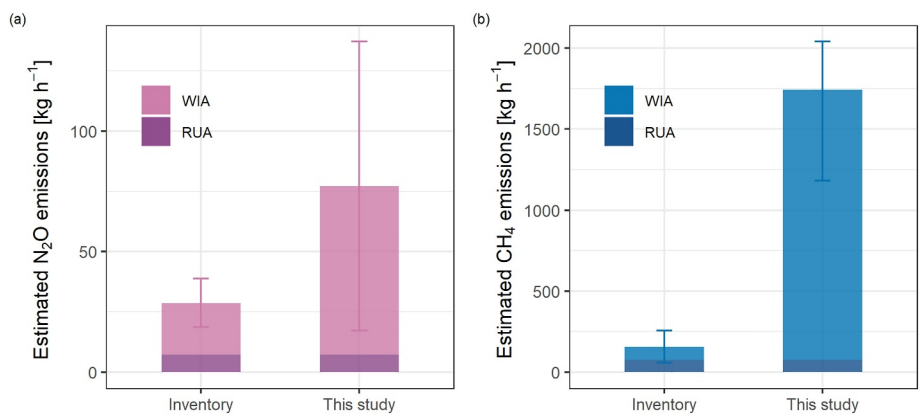

Figure 4. Panel (a, b) show the point sources' emissions of N_2O and CH_4 in the WIA and the RUA from the source categories of Chemical Industry, Energy, and Refineries as a group for the inventory and this study. The inventory represents yearly emissions, and the estimated emissions based on measurements in this study represent snap-shot emissions only. The uncertainties of inventory estimates were selected as the largest value of the uncertainties for different source categories in the national inventory report; the uncertainty of N_2O emission estimates in this study was calculated as the standard deviation of the mean of individual estimates, whereas the uncertainty of CH_4 emissions estimated from one day was inherently represented as the range of sensitivity test's results.

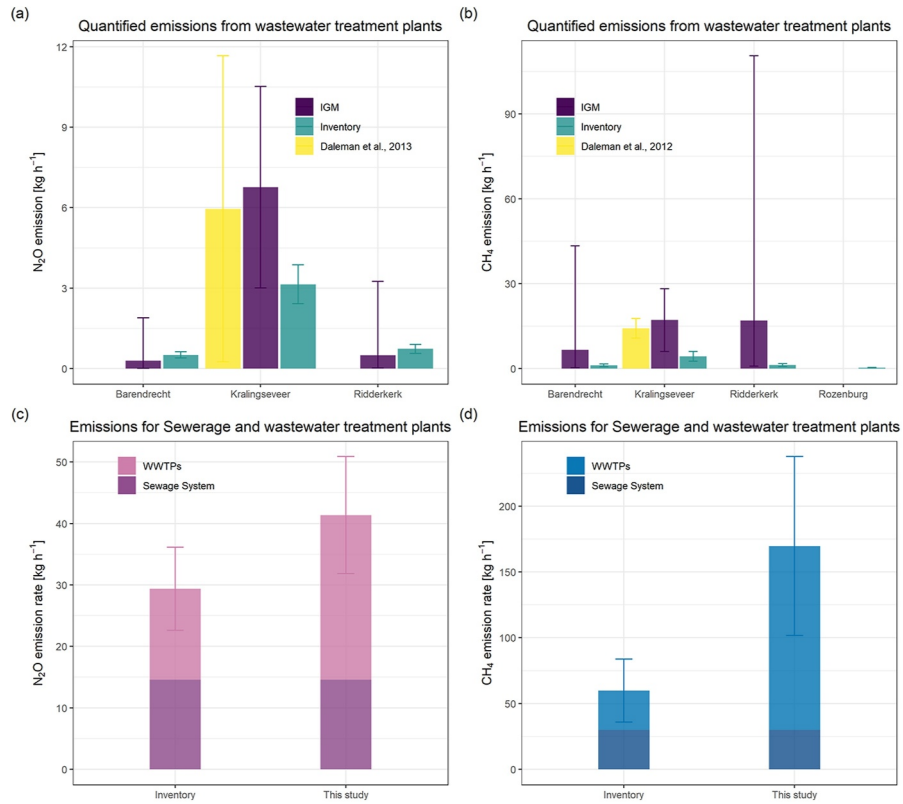

Figure 5. Panels (a, b) compare the estimated N_2O and CH_4 emissions for individual WWTPs in this study, the inventory, and the literature. The uncertainty of our estimated emissions was represented as the standard deviation of the mean for the WWTP with more than 10 transects and the range of 0.05–6.5 times the emissions for the WWTPs with only 1–2 transects according to previous study. Panels (c, d) indicate the N_2O and CH_4 emissions from the category Sewerage and Wastewater Treatment Plants over the entire Rotterdam area estimated by the inventory and this study with modified WWTPs' emissions based on observations and no modification of sewerage emissions.

IGM and are uncertain due to atmospheric variabilities (Caulton et al., 2018). The estimated emissions of N_2O and CH_4 using an IGM are shown in Figures 5a and 5b.

The estimated emissions of N_2O (6.7 kg hr^{-1}) and CH_4 (17.1 kg hr^{-1}) from the WWTP Kralingseveer are about 2 and 4 times the emissions of 3.1 kg hr^{-1} for N_2O and 4.3 kg hr^{-1} for CH_4 reported in the Dutch inventory, respectively. Many studies have found that the emissions of N_2O and CH_4 from WWTPs were underestimated in inventories (Moore et al., 2023). (Daelman, De Baets, et al., 2013; Daelman, van Voorthuizen, et al., 2013) collected directly off-gas leaving sludge reactors at four pipes with a controlled mass flow rate and derived emissions for the same WWTP Kralingseveer based on the measured concentrations of collected gas samples, and the mean emissions of 6 kg hr^{-1} and 14 kg hr^{-1} for N_2O and CH_4 are similar to our estimates. They found a seasonal variation of the estimated N_2O emissions with a peak showing up in March and low values in winter and no emissions for several weeks in November and December (Daelman et al., 2015) but not for CH_4 emissions (Daelman et al., 2012; Daelman, van Voorthuizen, et al., 2013). Our estimates represent N_2O emissions from the WWTP Kralingseveer during the period of August-September, and more measurements throughout the whole year should be performed to capture the seasonal variation. In addition, the estimated N_2O emissions from the WWTPs Barendrecht and Ridderkerk are a bit smaller than the emission reported in the Dutch inventory, whereas the estimated CH_4 emissions for the WWTPs plus Rozenburg are 6–23 times the inventory-based estimates. We upscaled the calculated emissions from the WWTPs to estimate the total emissions of N_2O and CH_4 from nine WWTPs in Rotterdam areas in spite of our limited data, and at the same time, the emissions from sewerage systems do not change. Our estimates allow for updating the inventory for the category of Sewerage and Wastewater Treatment Plants (Figure 5). The emission estimates derived by the IGM were found to have a high correlation ($r^2 = 0.9$) for N_2O and a moderate correlation ($r^2 = 0.5$) for CH_4 with the inventory estimates (Figure

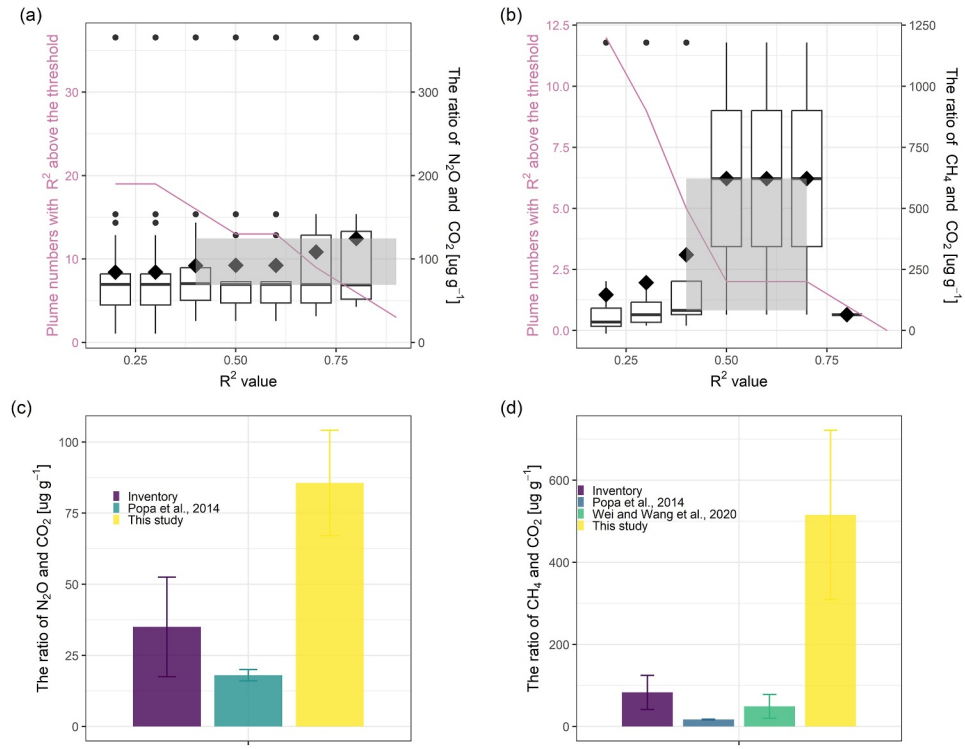

Figure 6. The statistics and relevant literature for tunnel measurements. The top panel shows the available numbers of plumes and the statistics of enhancement ratios against various r-squared values for (a) $\frac{\Delta N_2O}{\Delta CO_2}$ and (b) $\frac{\Delta CH_4}{\Delta CO_2}$; the box-plot encompasses the interquartile range from the 25th percentile to the 75th percentile with the median indicated by a horizontal line within the box, the points in a diamond shape indicate the mean of enhancement ratios, and the shaded area indicates the range that the mean and median of the ratios passing the criterion. The bottom panel compares the determined enhancement ratios in this study with the values in previous studies and the inventory for (c) $\frac{\Delta N_2O}{\Delta CO_2}$ and (d) $\frac{\Delta CH_4}{\Delta CO_2}$; the uncertainty of our estimated emissions was represented as the standard deviation of the mean, and the uncertainty of the inventory estimates was selected from the national inventory report for the source category of Traffic and Transportation.

S14 in Supporting Information S1) based on which the emissions from each WWTP can be derived. The total estimated emissions from WWTPs in the Rotterdam area of 26.8 kg hr^{-1} and 67.3 kg hr^{-1} for N_2O and CH_4 are 1.8 times and 2.2 times as large as the inventory estimates of 14.8 kg hr^{-1} and 29.9 kg hr^{-1}, respectively. In this study, the upscaled emissions are uncertain due to the limited number of investigated WWTPs and transects. Additional field measurements are required to quantify the emissions of N_2O and CH_4 from each WWTP more accurately and to verify inventories truthfully.

We analyzed the measured plume downwind of the WWTP Kralingseveer and the power plants (point sources categorized into energy). The concentration enhancements downwind of the WWTP show a high correlation for N_2O and CH_4 ($r^2 > 0.6$, the same for following descriptions about a high correlation), and each of them correlates with CO_2 (Figure S15 in Supporting Information S1). Besides, half of the observed plumes downwind of power plants show high correlations between N_2O and CO_2. This indicates N_2O is likely co-emitted not only with CH_4 during wastewater treatment processes but also with CO_2 from combustion for power production in a WWTP.

3.3. The N_2O and CH_4 Emissions for Traffic and Transportation

In total, 19 plumes were observed in different tunnels for the whole campaign, which were recognized to be caused by the emissions from Traffic and Transportation as there is hardly any perturbation by other emissions. The concentrations of N_2O and CO_2 were found to have a higher correlation than the concentrations of CH_4 and CO_2; 16 out of 19 plumes have a r-squared value above 0.4 for N_2O and CO_2, while only 5 out of 19 plumes for CH_4 and CO_2 (Figure 6; Table S4 and Figure S13 in Supporting Information S1). We have made sensitivity tests where varying r-squared values in the range of 0.4–0.8 were used as thresholds and found that the enhancement

Table 3
The Regional Emissions of N_2O and CH_4 in the WIA Estimated by the MBA for Individual Flights With Uncertainties Determined by Propagation of Individual Uncertainties of Concentration Enhancements and Meteorological Parameters

Species	Flight	Flux [kg·h^{-1}]
N_2O	0830	92 ± 79
	0901	103 ± 59
	0906	105 ± 50
CH_4	0906	1,970 ± 808

ratios between N_2O and CO_2 were rather stable, ranging from 84 to 125 μg N_2O/g CO_2, whereas the CH_4/CO_2 ratios show a large variation, ranging from 65 to 622 μg CH_4/g CO_2 as shown in the shaded area (Figure 6). The enhancement ratios in this study are much larger than the values of 18 ± 2 μg N_2O/g CO_2 and 17 ± 1 μg CH_4/g CO_2 measured from tunnels in Switzerland (Popa et al., 2014), and the value of 49 ± 29 μg CH_4/g CO_2 measured from tunnels in Shanghai, China (Wei & Wang, 2020). We speculate that the difference could originate from different catalyst converters for transforming N_2O to N_2 and different chemical compositions of fuels.

The average $\frac{\Delta N_2O}{\Delta CO_2}$ and $\frac{\Delta CH_4}{\Delta CO_2}$ of the plumes passing the criterion are 2.6–3.6 and 3.7 to 7.5 times the emission ratios of 35 μg N_2O/g CO_2 and 83 μg CH_4/g CO_2 that the inventory uses for Traffic and Transportation (Figure 6). We used the mean values as upscaling factors that are 2.9 and 5.5, respectively, to determine the emissions of N_2O and CH_4 for the whole category of Traffic and Transportation, which leads to estimates of 38.8 ± 8.4 kg hr^{-1} for N_2O and 175.7 ± 70.3 kg hr^{-1} for CH_4, respectively.

3.4. Reconciling the Top-Down and Bottom-Up Estimates

We derived top-down estimates of the total emissions for the whole Rotterdam area by summing up the estimated emissions for the WIA and the emissions for the RUA, which were estimated in our previous work (Tong et al., 2023). The estimated emissions using the MBA represent the regional emissions for the WIA integrating multiple sources' emissions. We present the estimated emissions on three individual days for N_2O and single day for CH_4 in Table 3. The estimated regional N_2O emissions are lower than the sum of point source emissions for flight 0830 (Table 1), and the discrepancy stems from systematic limitations in the MBA methodology. Our study employed upwind concentrations as background, an approach that is sensitive to temporal atmospheric changes, requires Lagrangian sampling conditions (tracking the same air mass) and is affected by boundary layer growth. As noted in the Text S2 in Supporting Information S1, our sampling was not conducted in a true Lagrangian framework, which likely resulted in upwind background concentrations being systematically higher than the actual downwind background concentrations (represented by low concentrations measured at the edges of the plume). This methodological limitation introduces substantial uncertainty into the mass balance estimates. Consequently, the MBA-derived regional emissions overlap with the point source emissions estimated by the WRF-LES model within their uncertainties, demonstrating that the apparent discrepancy falls within the expected uncertainty range of the MBA. The estimated regional N_2O emissions do not show large daily variations. The successful determination of CH_4 emissions in only one of four flights highlights an inherent detection bias in the aircraft-based MBA. Our previous work established the emission detection limits of the MBA (Tong et al., 2023), demonstrating that emissions below this threshold cannot be quantified using this method. Our emission estimate likely represents an upper-bound scenario rather than a temporal average, as the exact conditions that enable detection may systematically favor sampling during higher-emission periods. This detection bias must be considered when comparing the determined one snap-shot CH_4 emissions with annual emission inventory estimates.

We compared the revised bottom-up inventory with the integrated top-down estimates of N_2O and CH_4 emissions for the entire Rotterdam area. The top-down estimates are about 2 times the latest version of the revised bottom-up N_2O inventory but do not significantly differentiate from the CH_4 inventory within uncertainties (Figure 7). We narrowed the gap between the top-down and bottom-up estimates by 50% compared to our previous work in which the provisional version of the inventory was analyzed. The source categories we have quantified are all underestimated for both N_2O and CH_4 by the inventory, and the underestimation of the total emissions of the category group (Refineries, Energy, and Chemical Industry) made the most contributions towards reconciling the bottom-up and top-down estimates. Note that we only updated the emissions of these industrial plants located in the WIA and did not update those located in the RUA. If the emissions of the plants in the RUA were underestimated as well, the inventory estimates for these categories would be even higher.

Our efforts narrowed down the discrepancy between the top-down and bottom-up estimates; however, our results also suggest the remaining underestimation of N_2O emissions from other known sources such as sewerage and landfills and perhaps unknown sources that are not fully accounted for in the Dutch inventory. The different

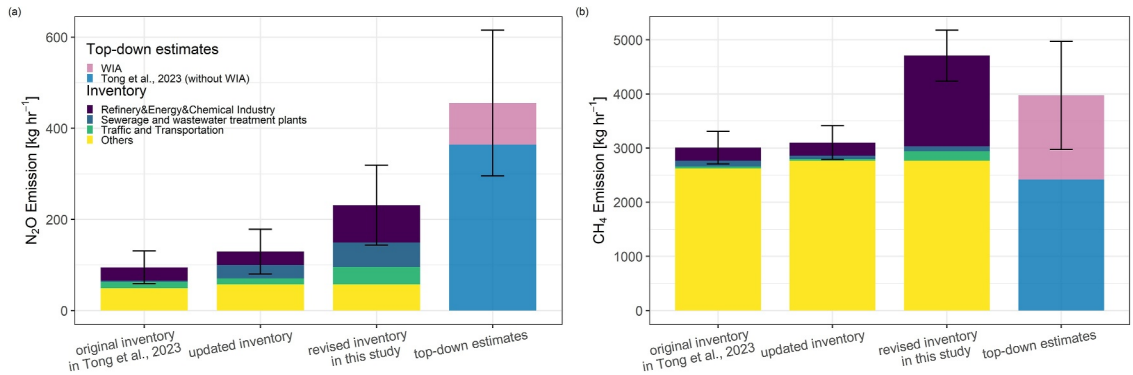

Figure 7. The comparison of the top-down estimates and different versions of the Dutch emission inventories for N_2O and CH_4 with uncertainties. In our previous work, we analyzed the provisional inventory, which was subsequently updated online. Based on this updated version, we derived a revised inventory in this study, which re-calculated the emissions for the group categories of Refineries, Energy, and Chemical Industry, the category Sewerage and Wastewater Treatment Plants, and the category Traffic and Transportation using atmospheric observations. The uncertainty of the inventory estimates was selected from the Dutch national inventory report, and the uncertainty of the top-down estimates was calculated from the uncertainties of the WIA and RUA areas' emission estimates using error propagation methods.

temporal representativeness of top-down estimates (hours) and bottom-up inventories (yearly average) should be considered when discussing the comparison results.

In this study, we could have quantified CH_4 emissions from multiple point sources scattered across Rotterdam if comprehensive concentration mapping data were available. Unlike large industrial facilities that behave as major point emitters, sources such as natural gas distribution systems, sewerage network systems, and heating furnaces of buildings are typically distributed across urban areas (Defratyka et al., 2021; Fernandez et al., 2022). These scattered sources have been successfully quantified using the approach proposed and improved by von Fischer et al. (2017) and Weller et al. (2018, 2019), which requires extensive concentration mapping of road networks throughout a city and applies empirical equations to determine emission rates. However, our mobile measurements were conducted only along the outermost circle of Rotterdam and therefore provided insufficient spatial coverage to apply this methodology effectively. If these distributed sources also emit N_2O, they could potentially be quantified using similar approaches. Future measurement campaigns should integrate various platforms and expand spatial coverage to better quantify emissions from multiple source types across Rotterdam, thereby improving both bottom-up inventory accuracy and the representativeness of top-down emission estimates.

4. Conclusions

We combined bottom-up and top-down methods to evaluate N_2O and CH_4 emissions in the Rotterdam area based on high-precision measurements made using an aircraft and a mobile vehicle. We derived top-down estimates for Rotterdam's total emissions by summing up the quantified west industrial area (WIA) emissions in this study and the determined Rotterdam urban area (RUA) emissions in our previous work. For the Dutch inventory, we revised the estimates for the categories of Sewerage and Wastewater Treatment Plants, Traffic and Transportation, Energy, Refineries, and Chemical Industry by replacing existing estimates with our newly quantified values. We find that the estimated N_2O emissions from WWTPs, industrial plants, and traffic and transportation are about 2–4 times the inventory estimates, whereas CH_4 emissions about 4–16 times the inventory estimates. The top-down estimates are consistent with the revised bottom-up inventories for CH_4 within uncertainties but about 2 times the inventory for N_2O, and the discrepancy has decreased by 50% compared to the original inventory analyzed in our previous work mainly due to the revision of industrial plants' emissions. However, conclusions must be interpreted cautiously due to the limited temporal representativeness of top-down estimates (hours) compared to bottom-up inventories (annual). We recommend combining top-down and bottom-up methods to provide complementary insights into urban emissions. To reconcile these estimates, comprehensive quantification across additional source categories and temporal scales is needed.

Conflict of Interest

The authors declare no conflicts of interest relevant to this study.

Data Availability Statement

The aircraft-based AirCore and ground-based mobile vehicle measurements were produced in the RITA (2022) campaign and can be accessed by requesting an API key after logging into the KNMI data platform at https://developer.dataplatform.knmi.nl/apis. The processed data from WRF-LES model output for comparison with airborne measurements are available at Zenodo https://doi.org/10.5281/zenodo.15482007. Data analysis and plot making are conducted by R 4.3.2, and the relevant code has been uploaded to GitHub and available at https://github.com/Xin0926/Rotterdam_N2O_CH4_emissions.

Acknowledgments
This work was supported by the National Key Research and Development Program of China under Grant 2022YFE0209100 and by the project of Youth Crossdisciplinary Team of the Chinese Academy of Sciences (No. 2023000126) and has been accomplished by using data generated in the Ruisdael Observatory, a scientific infrastructure co-financed by the Dutch Research Council (NWO, Grant 184.034.015). The authors would like to thank the General Electric Company and Gerben Bergman and Jan Willem Wagenaar from TNO for providing vertical profiles of meteorological parameters to validate the configuration of the WRF-LES model and Pim van de Bulk (TNO), Daniëlle van Dinther (TNO), and Ilona Velzeboer for driving the measurement van and performing calibrations of the instruments therein. We thank AER, and more specifically Hugo Denier van de Gon, for useful discussion about the Dutch emission inventory.

References

Addington, O., Zeng, Z.-C., Pongetti, T., Shia, R.-L., Gurney, K. R., Liang, J., et al. (2021). Estimating nitrous oxide (N_2O) emissions for the Los Angeles Megacity using mountaintop remote sensing observations. *Remote Sensing of Environment*, *259*(July 2020), 112351. https://doi.org/10.1016/j.rse.2021.112351

Ars, S., Vogel, F., Arrowsmith, C., Heerah, S., Knuckey, E., Lavoie, J., et al. (2020). Investigation of the spatial distribution of methane sources in the greater Toronto area using mobile gas monitoring systems. *Environmental Science & Technology*, *54*(24), 15671–15679. https://doi.org/10.1021/acs.est.0c05386

Barker, P. A., Allen, G., Flynn, M., Riddick, S., & Pitt, J. R. (2022). Measurement of recreational N_2O emissions from an urban environment in Manchester, UK. *Urban Climate*, *46*(July), 101282. https://doi.org/10.1016/j.uclim.2022.101282

Caulton, D. R., Li, Q., Bou-Zeid, E., Fitts, J. P., Golston, L. M., Pan, D., et al. (2018). Quantifying uncertainties from mobile-laboratory-derived emissions of well pads using inverse Gaussian methods. *Atmospheric Chemistry and Physics*, *18*(20), 15145–15168. https://doi.org/10.5194/acp-18-15145-2018

Charoenpornpukdee, K., Stanley, K., Pitt, J., Wenger, A., Manning, A., Young, D., et al. (2023). Recreational drug-use as an urban source of nitrous oxide. *Environmental Sciences: Atmosphere*, *3*(6), 962–969. https://doi.org/10.1039/D3EA00025G

Daelman, M. R. J., De Baets, B., van Loosdrecht, M. C. M., & Volcke, E. I. P. (2013). Influence of sampling strategies on the estimated nitrous oxide emission from wastewater treatment plants. *Water Research*, *47*(9), 3120–3130. https://doi.org/10.1016/j.watres.2013.03.016

Daelman, M. R. J., van Voorthuizen, E. M., van Dongen, L. G. J. M., Volcke, E. I. P., & van Loosdrecht, M. C. M. (2013). Methane and nitrous oxide emissions from municipal wastewater treatment—Results from a long-term study. *Water Science and Technology*, *67*(10), 2350–2355. https://doi.org/10.2166/wst.2013.109

Daelman, M. R. J., van Voorthuizen, E. M., van Dongen, U. G. J. M., Volcke, E. I. P., & van Loosdrecht, M. C. M. (2012). Methane emission during municipal wastewater treatment. *Water Research*, *46*(11), 3657–3670. https://doi.org/10.1016/j.watres.2012.04.024

Daelman, M. R. J., van Voorthuizen, E. M., van Dongen, U. G. J. M., Volcke, E. I. P., & van Loosdrecht, M. C. M. (2015). Seasonal and diurnal variability of N_2O emissions from a full-scale municipal wastewater treatment plant. *Science of the Total Environment*, *536*, 1–11. https://doi.org/10.1016/j.scitotenv.2015.06.122

Defratyka, S. M., Paris, J.-D., Yver-Kwok, C., Fernandez, J. M., Korben, P., & Bousquet, P. (2021). Mapping urban methane sources in Paris, France. *Environmental Science & Technology*, *55*(13), 8583–8591. https://doi.org/10.1021/acs.est.1c00859

Famulari, D., Nemitz, E., Di Marco, C., Phillips, G. J., Thomas, R., House, E., & Fowler, D. (2010). Eddy-covariance measurements of nitrous oxide fluxes above a city. *Agricultural and Forest Meteorology*, *150*(6), 786–793. https://doi.org/10.1016/j.agrformet.2009.08.003

Fernandez, J. M., Maazallahi, H., France, J. L., Menoud, M., Corbu, M., Ardelean, M., et al. (2022). Street-level methane emissions of Bucharest, Romania and the dominance of urban wastewater. *Atmospheric Environment: X*, *13*, 100153. https://doi.org/10.1016/j.aeaoa.2022.100153

Helfter, C., Tremper, A. H., Halios, C. H., Kotthaus, S., Bjorkegren, A., Grimmond, C. S. B., et al. (2016). Spatial and temporal variability of urban fluxes of methane, carbon monoxide and carbon dioxide above London, UK. *Atmospheric Chemistry and Physics*, *16*(16), 10543–10557. https://doi.org/10.5194/acp-16-10543-2016

Herrera, S. A., Diskin, G. S., Harward, C., Sachse, G., De Wekker, S. F. J., Yang, M., et al. (2021). Wintertime nitrous oxide emissions in the San Joaquin valley of California estimated from aircraft observations. *Environmental Science & Technology*, *55*(8), 4462–4473. https://doi.org/10.1021/acs.est.0c08418

Järvi, L., Nordbo, A., Rannik, Ü., Haapanala, S., Mammarella, I., Pihlatie, M., et al. (2014). Urban nitrous-oxide fluxes measured using the eddy-covariance technique in Helsinki, Finland. *Boreal Environment Research*, *19*(September), 108–121.

Karion, A., Ghosh, S., Lopez-Coto, I., Mueller, K., Gourdji, S., Pitt, J., & Whetstone, J. (2023). Methane emissions show recent decline but strong seasonality in two US northeastern cities. *Environmental Science & Technology*, *57*(48), 19565–19574. https://doi.org/10.1021/acs.est.3c05050

Klausner, T., Mertens, M., Huntrieser, H., Galkowski, M., Kuhlmann, G., Baumann, R., et al. (2020). Urban greenhouse gas emissions from the Berlin area: A case study using airborne CO_2 and CH_4 in situ observations in summer 2018. *Elementa: Science of the Anthropocene*, *8*(1), 15. https://doi.org/10.1525/elementa.411

Laskar, A. H., Soesanto, M. Y., & Liang, M.-C. (2021). Role of vehicular catalytic converter temperature in emission of pollutants: An assessment based on isotopic analysis of CO_2 and N_2O. *Environmental Science & Technology*, *55*(8), 4378–4388. https://doi.org/10.1021/acs.est.0c07430

Lavoie, T. N., Shepson, P. B., Gore, C. A., Stirm, B. H., Kaeser, R., Wulle, B., et al. (2017). Assessing the methane emissions from natural gas-fired power plants and oil refineries. *Environmental Science & Technology*, *51*(6), 3373–3381. https://doi.org/10.1021/acs.est.6b05531

Maazallahi, H., Fernandez, J. M., Menoud, M., Zavala-Araiza, D., Weller, Z. D., Schwietzke, S., et al. (2020). Methane mapping, emission quantification, and attribution in two European cities: Utrecht (NL) and Hamburg (DE). *Atmospheric Chemistry and Physics*, *20*(23), 14717–14740. https://doi.org/10.5194/acp-20-14717-2020

Manwell, J. F., McGowan, J. G., & Rogers, A. L. (2009). *Wind energy explained: Theory, design, and application* (2nd ed.). John Wiley & Sons, Ltd.

Moore, D. P., Li, N. P., Wendt, L. P., Castañeda, S. R., Falinski, M. M., Zhu, J.-J., et al. (2023). Underestimation of sector-wide methane emissions from United States wastewater treatment. *Environmental Science & Technology*, *57*(10), 4082–4090. https://doi.org/10.1021/acs.est.2c05373

Nogueira, T., Kamigauti, L. Y., Pereira, G. M., Gavidia-Calderón, M. E., Ibarra-Espinosa, S., Oliveira, G. L., et al. (2021). Evolution of vehicle emission factors in a megacity affected by extensive biofuel use: Results of tunnel measurements in São Paulo, Brazil. *Environmental Science & Technology*, *55*(10), 6677–6687. https://doi.org/10.1021/acs.est.1c01006

O'Shea, S. J., Allen, G., Fleming, Z. L., Bauguitte, S. J.-B., Percival, C. J., Gallagher, M. W., et al. (2014). Area fluxes of carbon dioxide, methane, and carbon monoxide derived from airborne measurements around Greater London: A case study during summer 2012. *Journal of Geophysical Research: Atmospheres*, *119*(8), 4940–4952. https://doi.org/10.1002/2013JD021269

Pitt, J. R., Allen, G., Bauguitte, S. J.-B., Gallagher, M. W., Lee, J. D., Drysdale, W., et al. (2019). Assessing London CO_2, CH_4 and CO emissions using aircraft measurements and dispersion modelling. *Atmospheric Chemistry and Physics*, *19*(13), 8931–8945. https://doi.org/10.5194/acp-19-8931-2019

Pitt, J. R., Lopez-Coto, I., Karion, A., Hajny, K. D., Tomlin, J., Kaeser, R., et al. (2024). Underestimation of thermogenic methane emissions in New York City. *Environmental Science and Technology*, *58*(21), 9147–9157. https://doi.org/10.1021/acs.est.3c10307

Popa, M. E., Vollmer, M. K., Jordan, A., Brand, W. A., Pathirana, S. L., Rothe, M., & Röckmann, T. (2014). Vehicle emissions of greenhouse gases and related tracers from a tunnel study: CO : CO_2, N_2O : CO_2, CH_4 : CO_2, O_2 : CO_2 ratios, and the stable isotopes ^{13}C and ^{18}O in CO_2 and CO. *Atmospheric Chemistry and Physics*, *14*(4), 2105–2123. https://doi.org/10.5194/acp-14-2105-2014

Ražnjević, A., van Heerwaarden, C., van Stratum, B., Hensen, A., Velzeboer, I., van den Bulk, P., & Krol, M. (2022). Technical note: Inter-pretation of field observations of point-source methane plume using observation-driven large-eddy simulations. *Atmospheric Chemistry and Physics*, *22*(10), 6489–6505. https://doi.org/10.5194/acp-22-6489-2022

RITA. (2022). The Ruisdael urban-atmosphere interactions intensive trace-gas and aerosol measurement campaign [Dataset]. *KNMI*. Retrieved from https://developer.dataplatform.knmi.nl/apis

Saide, P. E., Steinhoff, D. F., Kosovic, B., Weil, J., Downey, N., Blewitt, D., et al. (2018). Evaluating methods to estimate methane emissions from oil and gas production facilities using LES simulations. *Environmental Science & Technology*, *52*(19), 11206–11214. https://doi.org/10.1021/acs.est.8b01767

Sargent, M. R., Floerchinger, C., McKain, K., Budney, J., Gottlieb, E. W., Hutyra, L. R., et al. (2021). Majority of US urban natural gas emissions unaccounted for in inventories. *Proceedings of the National Academy of Sciences*, *118*(44), 2021. https://doi.org/10.1073/pnas.2105804118

Super, I., Denier van der Gon, H. A. C., Visschedijk, A. J. H., Moerman, M. M., Chen, H., van der Molen, M. K., & Peters, W. (2017). Interpreting continuous in-situ observations of carbon dioxide and carbon monoxide in the urban port area of Rotterdam. *Atmospheric Pollution Research*, *8*(1), 174–187. https://doi.org/10.1016/j.apr.2016.08.008

Tong, X. (2025). processed_data_from_output_WRF-LES_model [Dataset]. *Zenodo*. https://doi.org/10.5281/zenodo.15482007

Tong, X., van Heuven, S., Scheeren, B., Kers, B., Hutjes, R., & Chen, H. (2023). Aircraft-based AirCore sampling for estimates of N_2O and CH_4 emissions. *Environmental Science & Technology*, *57*(41), 15571–15579. https://doi.org/10.1021/acs.est.3c04932

USEPA. (1995). User's guide for the industrial source complex (ISC3) dispersion model (Vol. *II*).

van der Net, L., Staats, N., Coenen, P. W. H. G., Rienstra, J. D., Zijlema, P. J., Arets, E. J. M. M., et al. (2024). *Greenhouse gas emissions in the Netherlands 1990-2022*. National Inventory Report 2024. https://doi.org/10.21945/RIVM-2024-0017

von Fischer, J. C., Cooley, D., Chamberlain, S., Gaylord, A., Griebenow, C. J., Hamburg, S. P., et al. (2017). Rapid, vehicle-based identification of location and magnitude of urban natural gas pipeline leaks. *Environmental Science & Technology*, *51*(7), 4091–4099. https://doi.org/10.1021/acs.est.6b06095

Wei, C., & Wang, M. (2020). Spatial distribution of greenhouse gases (CO_2 and CH_4) on expressways in the megacity Shanghai, China. *Environmental Science and Pollution Research*, *27*(25), 31143–31152. https://doi.org/10.1007/s11356-020-09372-1

Weller, Z. D., Roscioli, J. R., Daube, W. C., Lamb, B. K., Ferrara, T. W., Brewer, P. E., & von Fischer, J. C. (2018). Vehicle-based methane surveys for finding natural gas leaks and estimating their size: Validation and uncertainty. *Environmental Science & Technology*, *52*(20), 11922–11930. https://doi.org/10.1021/acs.est.8b03135

Weller, Z. D., Yang, D. K., & von Fischer, J. C. (2019). An open source algorithm to detect natural gas leaks from mobile methane survey data. *PLoS One*, *14*(2), e0212287. https://doi.org/10.1371/journal.pone.0212287

Williams, J. P., Ars, S., Vogel, F., Regehr, A., & Kang, M. (2022). Differentiating and mitigating methane emissions from fugitive leaks from natural gas distribution, historic landfills, and manholes in Montréal, Canada. *Environmental Science and Technology*, *56*(23), 16686–16694. https://doi.org/10.1021/acs.est.2c06254